Anomalous Transport through the *p*-Wave Superconducting Channel in the 3-K Phase of Sr_2RuO_4

Hiroshi Kambara,[1] Satoshi Kashiwaya,[1] Hiroshi Yaguchi,[2] Yasuhiro Asano,[3] Yukio Tanaka,[4] and Yoshiteru Maeno[5]

[1]*National Institute of Advanced Industrial Science and Technology (AIST), Tsukuba 305-8568, Japan*
[2]*Department of Physics, Faculty of Science and Technology, Tokyo University of Science, Noda 278-8510, Japan*
[3]*Department of Applied Physics, Hokkaido University, Sapporo 060-8628, Japan*
[4]*Department of Applied Physics, Nagoya University, Nagoya 464-8603, Japan*
[5]*Department of Physics, Kyoto University, Kyoto 606-8502, Japan*
(Received 8 July 2008; published 30 December 2008)

Using microfabrication techniques, we extracted individual channels of 3-kelvin (3-K) phase superconductivity in Sr_2RuO_4-Ru eutectic systems and confirmed odd-parity superconductivity in the 3-K phase, similar to pure Sr_2RuO_4. Unusual hysteresis in the differential resistance-current and voltage-current characteristics observed below 2 K indicates the internal degrees of freedom of the superconducting state. A possible origin of the hysteresis is current-induced chiral-domain-wall motion due to the chiral *p*-wave state.

DOI: 10.1103/PhysRevLett.101.267003 PACS numbers: 74.70.Pq, 74.25.Sv, 74.45.+c, 74.81.−g

Most superconductors have a spin-singlet pairing state, including high-T_c cuprates. Spin-triplet pairing superconductors are quite rare, and the superconducting transition temperature (T_c) is generally low (~1 K). Layered perovskite Sr_2RuO_4 (SRO) is one of the best candidates for spin-triplet pairing with a T_c of 1.5 K, and the superconducting vector order parameter is similar to that of the superfluid ^{3}He-*A*—the so-called chiral *p*-wave state [1]. The pure SRO phase (1.5-K phase) has been well studied, but SRO-Ru eutectics in which Ru lamellae are embedded are not well understood. The SRO-Ru eutectic is called the 3-kelvin (3-K) phase [2–4] because of the remarkable enhancements of T_c up to 3 K. However, the enhancement mechanism of T_c and the pairing symmetry of the 3-K phase have not been understood clearly. Since the 3-K phase is the interface superconductivity in the SRO region between SRO and Ru [4], the volume fraction of the superconducting state is very low compared with that of the pure phase. Thus, it is difficult to determine the pairing symmetry by the ordinary method, i.e., Knight shift by NMR. It is extremely important to determine the pairing symmetry of the 3-K phase, because T_c of 3 K is the highest among spin-triplet superconductors if the 3-K phase is established as a spin-triplet superconductor. Moreover, the 3-K phase enables us to reveal nanoscale physics in inhomogeneous spin-triplet superconductivity.

Thus far, several experiments have been performed to investigate the pairing symmetry of the 3-K phase. In tunnel junction experiments, Mao *et al.* [5] and Kawamura *et al.* [6] observed the zero-bias conductance peak due to Andreev resonance reflecting *non-s*-wave superconductivity [7]. Hooper *et al.* [8] reported the *c*-axis transport characteristics, which is interpreted in terms of a complex Josephson network with anomalous asymmetric features in their current-voltage characteristics. Although these results imply an internal phase of the superconducting order parameter, they do not necessarily indicate odd-parity superconductivity of the 3-K phase.

In this study, we investigated the *ab*-plane differential resistance-current (dV/dI-I) and voltage-current (V-I) characteristics of the 3-K phase by controlling the number of Ru inclusions by a microfabrication technique using a focused ion beam (FIB). We extracted individual channels which connect the 3-K phase region–normal-state region of the SRO–3-K phase region as the superconductor–normal-metal–superconductor junction at $3\ \mathrm{K} > T > 1.5\ \mathrm{K}$ [Fig. 1(b)]. We then determine the pairing symmetry of the 3-K phase from the temperature dependence of the critical current (I_c). Finally, we show quite unusual hysteresis in dV/dI-I and V-I below 2 K, which strongly indicates the internal degrees of freedom, possibly due to the chiral *p*-wave state.

Eutectic crystals of SRO-Ru were grown in an infrared image furnace by the floating zone method [9]. The transport was measured using a standard four-probe technique. The sample neck between the voltage-lead contacts was milled by a FIB to reduce the number of Ru inclusions in this region. The details of the sample preparation and measurement system are described elsewhere [10]. For sample A, the neck region was $70 \times 70 \times 35\ \mu\mathrm{m}^3$ (sample A-1) before the FIB process [Fig. 1(a), top]. Next, it was successively milled narrower and thinner (samples A-2 → A-3). The final dimensions of the neck were $20 \times 20 \times (<10)\ \mu\mathrm{m}^3$ (sample A-3) [Fig. 1(a), bottom]. In Fig. 1(c), ~1 μm thick and 1–6 μm long Ru inclusions are visible as black bars. Only two pieces of Ru inclusions appear on the topmost surface in the neck region of sample A-3. Thus, there should be only a few Ru inclusions in the neck region, including a few hidden below the surface. Figure 1(d) shows the differential resistance at zero-bias current (R)-temperature curves of samples A-1, 2, and 3, respectively. For clarity, R is normalized at 4.2 K,

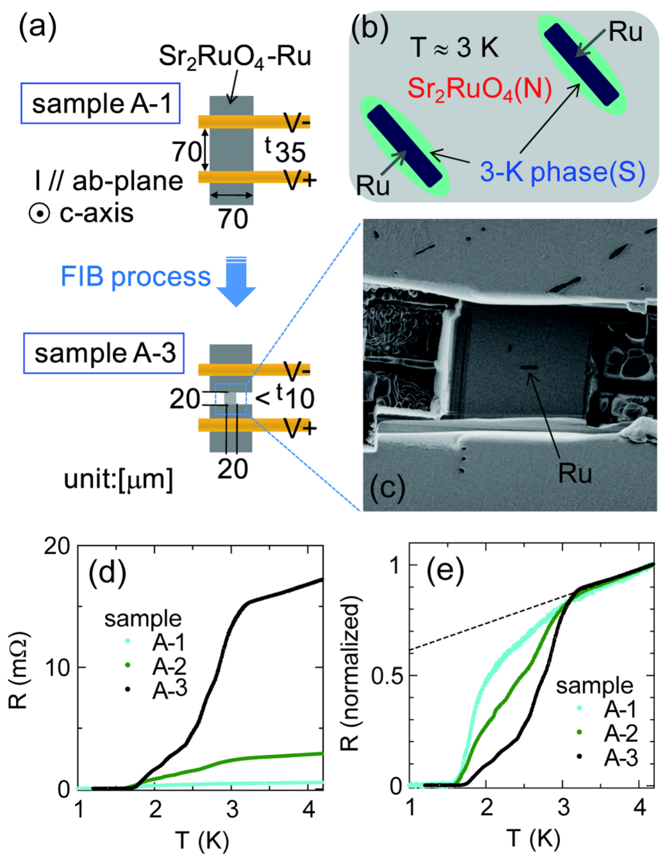

FIG. 1 (color online). Sketch of the sample configurations for samples A-1 [(a), top] and A-3 [(a), bottom] of Sr_2RuO_4-Ru. Sample A-3 was milled by a FIB. (b) Schematic image of nucleation of the 3-K phase superconductivity around Ru inclusions at 3 K. (c) Scanning ion microscope image ($50 \times 50\ \mu m^2$) of sample A-3. The black bars show the Ru inclusions. (d) Zero-bias differential resistance (R) vs temperature for samples A-1, A-2, and A-3. (e) Normalized resistance at 4.2 K vs T. The dashed line represents a normal component.

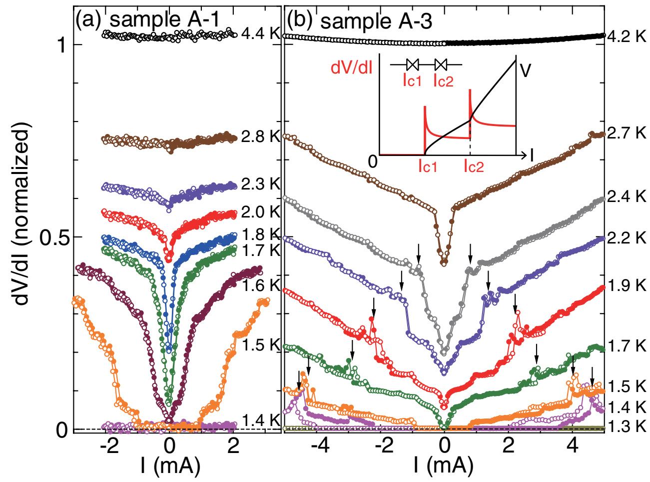

FIG. 2 (color online). Normalized dV/dI vs I as a function of temperature for samples A-1 (a) and A-3 (b), respectively. The open and solid symbols denote the different sweep directions, from zero to max. (open), max. to min. (solid), and min. to zero (open). A series of the most pronounced kinks are denoted by arrows (average currents of the dV/dI peaks in upward and downward sweep directions). Inset: Characteristic kinks in the dV/dI-I curves are explained by superconducting linkage channels with critical currents ($I_{c1} < I_{c2} < \cdots$) in series. The red (black) line corresponds to a schematic of dV/dI-I (V-I).

as shown in Fig. 1(e). We can see that the component of the 3-K phase is more dominant in sample A-3 than in sample A-1. Thus, the milling process can change the ratio of the 1.5-K:3-K phase. Note that it is not always the case that the component of the 3-K phase becomes dominant by milling.

In Figs. 2(a) and 2(b), we show dV/dI-I curves normalized to 4.2 K for samples A-1 and A-3. Below ~3 K, dV/dI curves show dip structures ($dV/dI \to 0$) near the zero-bias current, reflecting the 3-K phase superconductivity. Below 1.6 K, the dV/dI curves show the flat zero resistance, reflecting the 1.5-K phase superconductivity in addition to a path formation due to the proximity effect of the 3-K phase superconductivity. Increasing the bias currents beyond some critical values makes the dV/dI values larger. In particular, for sample A-3, more characteristic kinks were observed in the dV/dI curves than for sample A-1. With a filament (nonuniform) model in which local superconducting channels connect Ru islands, the characteristic kinks are naturally explained by the superconducting linkage channels in series with their own critical currents, as illustrated in the inset in Fig. 2(b). Thus we can extract the I_c of each channel for sample A-3. In sample A, it is difficult to separate the channels without FIB milling possibly because similar linkage channels are averaged; i.e., sample A-1 hides the individuality of the channels.

Figure 3 shows the temperature dependence of I_c focusing only on the most pronounced kinks [the arrows in Fig. 2(b)] for three different types of samples cut from

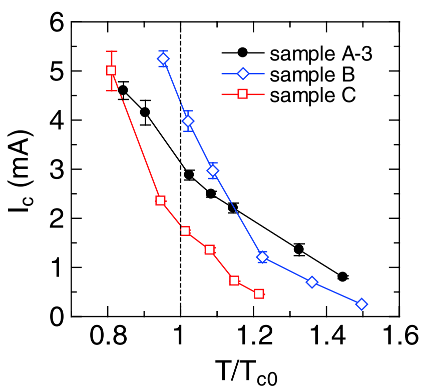

FIG. 3 (color online). Critical currents (I_c) vs normalized temperature for samples A-3, B, and C, respectively. The three curves are traces of the most pronounced kinks in each series of dV/dI-I curves [for sample A-3, the arrows in Fig. 2(b)].

the same crystal rod. A continuous monotonic increase is seen in the value of I_c with the temperature decreasing through T_{c0} which is defined as the zero-resistivity point in Figs. 1(d) and 1(e). The temperature dependence of I_c should reflect the relationship of the pairing symmetry of the 3-K and 1.5-K phases. From the experiment by Jin and co-workers [11], I_c of Josephson junctions (JJs) in Pb-SRO-Pb increases below 7.2 K (T_c of Pb) with decreasing temperature but decreases below 1.3 K (T_c of SRO). This result is explained by the transition from 0 to the π junction, which forms below 1.3 K due to the difference in parity of the pairing symmetry (Pb has s-wave and SRO has p-wave pairing symmetry) either as a first-order [12] or a second-order process [13]. Assuming a similar relation, we deduce that the 3-K and 1.5-K phases have the same parity, such as s-s-s or p-p-p in the 3-K–1.5-K–3-K phase configuration, excluding π-junction configurations. Therefore, considering an odd parity in the 1.5-K phase, the 3-K phase also has an odd parity in the local superconducting channel. This is an experimental proof of the assumption in a phenomenological theory by Sigrist and Monien (SM) [14], which states that the filamentary phase at 3 K has p-wave pairing symmetry.

In the dV/dI-I curves, we observed unusual hysteresis below 2 K, as seen for sample A-3 [Fig. 2(b)]. The hysteresis curves are more pronounced at temperatures below T_{c0} and tend to appear for small samples after FIB milling. To demonstrate the anomalous behavior in $dV/dI - I$ data clearly, we show V-I curves obtained by the dc method as well as dV/dI-I curves for sample D (the neck region is $3 \times 10 \times 5\ \mu\text{m}^3$[(width) $\times$ (length) $\times$ (thickness)]) at 1.3 K in Figs. 4(a) and 4(b). The V-I data show discontinuous points at ± 3 and ± 4.3 mA when sweeping up of absolute value of the dc current [Fig. 4(a)]. To explain this behavior, we show a schematic of the V-I data in Fig. 4(c). When we increase the dc current from 0, a finite voltage appears at I_{c0} like usual JJs. Here the I_{c0} is defined as a critical current at which a finite dV/dI value is observed. Surprisingly, the voltage suddenly drops at a threshold $I_{\rm th1} > I_{c0}$ denoted by the arrow. With further increasing of the dc current, a similar voltage drop appears at $I_{\rm th2}$. We note that one can measure only positive dV/dI by the ac method [Fig. 4(b)] because the switching occurs instantaneously at $I_{\rm th1}$, $I_{\rm th2}$, etc. That is, the dV/dI value around the threshold reflects that just before the switching or just after the switching.

Here we emphasize that $I_{\rm th}$ is *not* a critical current from the dc to ac Josephson effect as seen in the inset in Fig. 2(b) because of the following anomalous features. (i) At $I_{\rm th}$, the voltage discontinuously *decreases* when the V-I curve switches to the next branch. (ii) It switches to a *lower-*R_n (normal resistance) branch that has a larger I_c. (iii) The hysteresis loop shows the opposite direction compared to typical JJs. In serially connected typical JJs, e.g., the c-axis intrinsic JJs of high-T_c cuprate $Bi_2Sr_2CaCu_2O_{8+\delta}$ [15], the

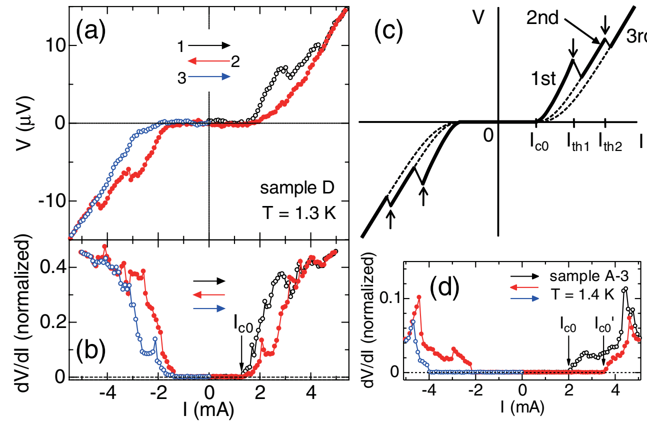

FIG. 4 (color online). (a) V-I characteristics at 1.3 K obtained by the dc method for sample D. The curves are obtained by averaging over 10 curves. The open and solid symbols denote the different sweep directions, from zero to max. (open black), max. to min. (solid red), and min. to zero (open blue). (b) Normalized dV/dI-I curves obtained by the ac method for sample D. (c) Schematic V-I characteristics. At $I_{\rm th1}$ ($I_{\rm th2}$), the V-I curve switches from the 1st (2nd) to the 2nd (3rd) branch when the dc current is swept up. When the dc current is swept down, the V-I curve follows the 3rd branch. (d) Normalized dV/dI-I curves at 1.4 K for sample A-3. I_{c0} and I'_{c0} are critical currents when dc currents are swept up and down, respectively.

voltage absolutely increases and R_n becomes larger after the zero-voltage state changes to the finite-voltage state. Furthermore, in typical JJs, I_c when sweeping up from 0 is *always* higher than I'_{c0} when sweeping down [16], which is obviously contrary to the data shown in Fig. 4(d). Therefore, the anomalous switchings at $I_{\rm th}$ above I_c are never explained in terms of serially connected JJs. In other words, the anomalous switching phenomena occur in the *identical* channel. Thus, it cannot be explained without considering the internal degrees of freedom of the superconducting state.

One of the possible explanations of the unusual hysteresis is due to the chirality of the superconducting state taking account of the 1.5-K phase being a chiral p-wave ($p_x \pm ip_y$) superconductor. The chiral state has two types of distinct domains in the superconducting state. If a superconducting linkage is formed from two antiparallel domains, there should exist a domain wall (DW) between them. No DW is formed between parallel domains. Let us assume that a local linkage channel contains both parallel and antiparallel domains, as depicted in Fig. 5. Each critical current is expected to be proportional to each cross section, i.e., $I_c \propto S_{\rm filament}$ or $I_c \propto S_{\rm DW}$, where $S_{\rm filament}$ is the cross section at which a weak link forms between parallel domains and $S_{\rm DW}$ is that between antiparallel domains. Generally, a DW is likely to be formed and pinned at defects in the sample. Once a DW forms, dc current which transfers a Cooper pair with a given chiral state ($p_x - ip_y$) to the opposite chiral state ($p_x + ip_y$) induces the DW

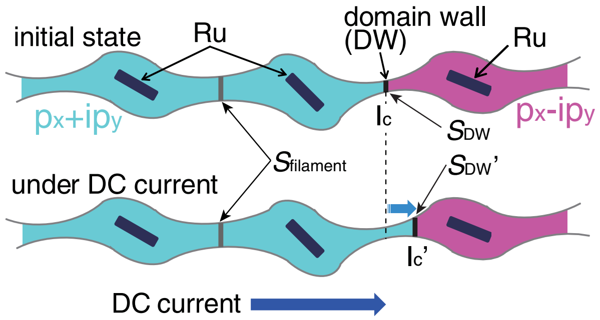

FIG. 5 (color online). Model of the chiral-domain-wall motion, induced by dc current. I_c and I_c' are critical currents when dc currents are swept up and down, respectively.

motion as a backaction. Assuming the spatial variation of the cross section of the linkage channel, the movement of the DW varies I_c during the current sweep. If the DW is pinned at defects at low-bias currents, the DW slides to the next metastable position when the dc current beyond the threshold [I_{th1}, I_{th2}, etc., in Fig. 4(c)] is applied. Thus, the branch of the V-I curve switches, which causes the anomalous hysteresis. As a small S_{DW} should be energetically favorable because the different order parameters overlap each other at the DW, it is reasonable that I_{c0} is lower than I_{c0}'. On the other hand, no hysteresis would appear in a channel between parallel domains without a DW. In short, the dV/dI-I curve shows two types: no hysteresis without a DW and hysteresis with a DW moving in alternate directions. The DW motion is analogous to the current-driven DW motion in magnetic wires [17]. Here we note that the chiral domain picture is consistent with the SM's prediction of the 2nd transition at T_2^* (3 K $> T_2^* >$ 1.5 K) with time reversal symmetry breaking. We also note that no hysteresis has been reported [8], possibly because I_c of averaged channels smeared it under a large number of Ru inclusions.

Recent Kerr effect [18] and JJ [19] experiments suggest the presence of the chiral domains for the 1.5-K phase. However, the estimated domain size is ~50–100 μm [18] and ~1 μm [19], respectively. Thus, a consensus about the domain size is not established yet. In our experiment for the 3-K phase, we estimate the domain size to be ~10 μm from the neck region of the sample if the chiral domain scenario is correct. We emphasize that our four-probe configuration is not sensitive to surface or interface states. Thus, our result reflects the intrinsic properties of the superconducting state in SRO removing experimental ambiguity as much as possible. Further experimental work is needed to verify the presence of the chiral domains in the 3-K phase and make further discussions about the effects of the chiral domains on the Josephson current [20].

In summary, we revealed the superconducting nature of the 3-K phase in Sr_2RuO_4 by transport measurements on microfabricated samples. We confirmed that the 3-K phase has odd-parity pairing symmetry, similar to the 1.5-K phase, from the monotonic temperature dependence of the critical currents. The unusual hysteresis of the differential resistance or the voltage-current characteristics in the sweeping current observed below 2 K indicates the internal degrees of freedom of the superconducting pairing, i.e., the chiral $p_x \pm ip_y$ state. The domain wall motion induced by the dc current is a possible origin of the hysteresis. This is a new discovery of the dynamic response of the superconducting order parameter of Sr_2RuO_4.

We are very grateful to T. Matsumoto for technical support. This work was financially supported by a Grant-in-Aid for Scientific Research on Priority Areas (No. 17071007) from MEXT, Japan.

[1] A. P. Mackenzie and Y. Maeno, Rev. Mod. Phys. **75**, 657 (2003).
[2] Y. Maeno *et al.*, Phys. Rev. Lett. **81**, 3765 (1998).
[3] T. Ando *et al.*, J. Phys. Soc. Jpn. **68**, 1651 (1999).
[4] H. Yaguchi *et al.*, Phys. Rev. B **67**, 214519 (2003).
[5] Z. Q. Mao *et al.*, Phys. Rev. Lett. **87**, 037003 (2001).
[6] M. Kawamura *et al.*, J. Phys. Soc. Jpn. **74**, 531 (2005).
[7] Y. Tanaka and S. Kashiwaya, Phys. Rev. Lett. **74**, 3451 (1995).
[8] J. Hooper *et al.*, Phys. Rev. B **70**, 014510 (2004).
[9] Z. Q. Mao, Y. Maeno, and H. Fukazawa, Mater. Res. Bull. **35**, 1813 (2000).
[10] H. Kambara *et al.*, Physica C (Amsterdam) (to be published).
[11] R. Jin *et al.*, Phys. Rev. B **59**, 4433 (1999).
[12] C. Honerkamp and M. Sigrist, Prog. Theor. Phys. **100**, 53 (1998).
[13] M. Yamashiro, Y. Tanaka, and S. Kashiwaya, J. Phys. Soc. Jpn. **67**, 3364 (1998).
[14] M. Sigrist and H. Monien, J. Phys. Soc. Jpn. **70**, 2409 (2001).
[15] For example, H. Kashiwaya *et al.*, J. Phys. Soc. Jpn. **77**, 104708 (2008), and references therein.
[16] A. Barone and G. Paternò, *Physics and Applications of the Josephson Effect* (Wiley, New York, 1982), Chap. 6.
[17] A. Yamaguchi *et al.*, Phys. Rev. Lett. **92**, 077205 (2004).
[18] J. Xia *et al.*, Phys. Rev. Lett. **97**, 167002 (2006).
[19] F. Kidwingira *et al.*, Science **314**, 1267 (2006).
[20] Y. Asano *et al.*, Phys. Rev. B **71**, 214501 (2005).